AFRL-ML-WP-TP-2007-497

STIMULATED PHOTOREFRACTIVE BACKSCATTER LEADING TO SIX-WAVE MIXING AND PHASE CONJUGATION IN IRON DOPED LITHIUM NIOBATE (PREPRINT)

D.R. Evans

Hardened Materials Branch
Survivability and Sensor Materials Division

APRIL 2007

AIR FORCE RESEARCH LABORATORY
MATERIALS AND MANUFACTURING DIRECTORATE
WRIGHT-PATTERSON AIR FORCE BASE, OH 45433-7750
AIR FORCE MATERIEL COMMAND
UNITED STATES AIR FORCE

NOTICE AND SIGNATURE PAGE

Using Government drawings, specifications, or other data included in this document for any purpose other than Government procurement does not in any way obligate the U.S. Government. The fact that the Government formulated or supplied the drawings, specifications, or other data does not license the holder or any other person or corporation; or convey any rights or permission to manufacture, use, or sell any patented invention that may relate to them.

This report was cleared for public release by the Air Force Research Laboratory Wright Site (AFRL/WS) Public Affairs Office and is available to the general public, including foreign nationals. Copies may be obtained from the Defense Technical Information Center (DTIC) (http://www.dtic.mil).

AFRL-ML-WP-TP-2007-497 HAS BEEN REVIEWED AND IS APPROVED FOR PUBLICATION IN ACCORDANCE WITH ASSIGNED DISTRIBUTION STATEMENT.

*//Signature//

DEAN R. EVANS, Ph.D.
Agile Filters Project
Exploratory Development
Hardened Materials Branch

//Signature//

MARK S. FORTE, Acting Chief
Hardened Materials Branch
Survivability and Sensor Materials Division

//Signature//

TIM J. SCHUMACHER, Chief
Survivability and Sensor Materials Division

This report is published in the interest of scientific and technical information exchange, and its publication does not constitute the Government's approval or disapproval of its ideas or findings.

*Disseminated copies will show "//Signature//" stamped or typed above the signature blocks.

REPORT DOCUMENTATION PAGE

Form Approved
OMB No. 0704-0188

1. REPORT DATE *(DD-MM-YY)*	2. REPORT TYPE	3. DATES COVERED *(From - To)*
April 2007	Journal Article Preprint	

4. TITLE AND SUBTITLE

STIMULATED PHOTOREFRACTIVE BACKSCATTER LEADING TO SIX-WAVE MIXING AND PHASE CONJUGATION IN IRON DOPED LITHIUM NIOBATE (PREPRINT)

5a. CONTRACT NUMBER
In-house

5b. GRANT NUMBER

5c. PROGRAM ELEMENT NUMBER
62102F

6. AUTHOR(S)

M.A. Saleh (UES, Inc.)
P.P Banerjee (University of Dayton)
J. Carns (General Dynamics Information Technology, Inc., formerly Anteon Corp.)
G. Cook (Universal Technology Corporation)
D.R. Evans (AFRL/MLPJ)

5d. PROJECT NUMBER
4348

5e. TASK NUMBER
RG

5f. WORK UNIT NUMBER
M08R1000

7. PERFORMING ORGANIZATION NAME(S) AND ADDRESS(ES)

UES, Inc.
4401 Dayton-Xenia Road,
Dayton, OH 45432

University of Dayton
Department of Electrical and Computer Engineering
Dayton, OH 45469

General Dynamics Information Technology, Inc.
5100 Springfield Pike, Suite 509
Dayton, OH 45431

Universal Technology Corporation
1270 North Fairfield Road
Dayton, OH 45432

Hardened Materials Branch (AFRL/MLPJ)
Survivability and Sensor Materials Division
Materials and Manufacturing Directorate
Wright-Patterson Air Force Base, OH 45433-7750
Air Force Materiel Command, United States Air Force

8. PERFORMING ORGANIZATION REPORT NUMBER
AFRL-ML-WP-TP-2007-497

9. SPONSORING/MONITORING AGENCY NAME(S) AND ADDRESS(ES)

Air Force Research Laboratory
Materials and Manufacturing Directorate
Wright-Patterson Air Force Base, OH 45433-7750
Air Force Materiel Command
United States Air Force

10. SPONSORING/MONITORING AGENCY ACRONYM(S)
AFRL/MLPJ

11. SPONSORING/MONITORING AGENCY REPORT NUMBER(S)
AFRL-ML-WP-TP-2007-497

12. DISTRIBUTION/AVAILABILITY STATEMENT
Approved for public release; distribution unlimited.

13. SUPPLEMENTARY NOTES
Journal article submitted to Applied Optics. The U.S. Government is joint author of this work and has the right to use, modify, reproduce, release, perform, display, or disclose the work. PAO Case Number: AFRL/WS 07-0775, 03 Apr 2007.

14. ABSTRACT

Oblique incidence of a 532 nm pump on $LiNbO_3$:Fe, nominally propagating along the +c axis, produces six waves through two-wave coupling (self diffraction) and four-wave mixing (parametric diffraction). One of these waves the stimulated photorefractive backscatter, contains the self-phase conjugate. The dynamics of six-wave mixing and their dependence on crystal parameters and angle of incidence are analyzed. A novel order analysis of the interaction equations provides further insight into experimental observations. The quality of the backscatter is evaluated through image restoration, interference experiments, and visibility measurement. Reduction of two-wave coupling may significantly improve the quality of the self-phase conjugate.

15. SUBJECT TERMS
Photorefractive, Phase Conjugate, $LiNbO_3$:Fe, Six-Wave mixing

16. SECURITY CLASSIFICATION OF:			17. LIMITATION OF ABSTRACT:	18. NUMBER OF PAGES	19a. NAME OF RESPONSIBLE PERSON (Monitor)
a. REPORT	b. ABSTRACT	c. THIS PAGE			Dean R. Evans
Unclassified	Unclassified	Unclassified	SAR	28	19b. TELEPHONE NUMBER *(Include Area Code)* N/A

Standard Form 298 (Rev. 8-98)
Prescribed by ANSI Std. Z39-18

Stimulated Photorefractive Backscatter Leading to Six-wave Mixing and Phase Conjugation in Iron Doped Lithium Niobate

M. A. Saleh
Air Force Research Laboratory, Materials and Manufacturing Directorate, WPAFB, OH 45433
UES, Inc., 4401 Dayton-Xenia Road, Dayton, Ohio 45432

P. P. Banerjee
Department of Electrical and Computer Engineering, University of Dayton, Dayton OH 45469

J. Carns
Air Force Research Laboratory, Materials and Manufacturing Directorate, WPAFB, OH 45433
Anteon Corporation, 5100 Springfield Pike, Suite 509, Dayton, Ohio 45431

G. Cook
Air Force Research Laboratory, Materials and Manufacturing Directorate, WPAFB, OH 45433
Universal Technology Corporation, 1270 North Fairfield Road, Dayton, Ohio 45432

D. R. Evans
Air Force Research Laboratory, Materials and Manufacturing Directorate, WPAFB, OH 45433

Abstract: Oblique incidence of a 532 nm pump on $LiNbO_3$:Fe, nominally propagating along the +c axis, produces six waves through two-wave coupling (self diffraction) and four-wave mixing (parametric diffraction). One of these waves, the stimulated photorefractive backscatter, contains the self-phase conjugate. The dynamics of six-wave mixing, and their dependence on crystal parameters and angle of incidence are analyzed. A novel order analysis of the interaction equations provides further insight into experimental observations. The quality of the backscatter is evaluated through image restoration, interference experiments, and visibility measurement. Reduction of two-wave coupling may significantly improve the quality of the self-phase conjugate.

Key Words: Photorefractive, phase conjugate, $LiNbO_3$:Fe, six-wave mixing, four-wave mixing, two-beam coupling, stimulated backscatter, coherence.
OCIS Codes: 190.7070 Two-wave mixing, 190. 5330 Four-wave mixing, 190.4380 Photorefractive Nonlinear Optics, 190.5040 Phase conjugation

1. Introduction

Stimulated photorefractive backscatter (SPBS) has been of significant interest in the area of photorefractive (PR) research. In particular, PR backscatter leading to phase conjugation processes have been theoretically and experimentally studied in various contexts.[1-7] In this paper, we report on SPBS in PR $LiNbO_3$ for a specific experimental arrangement that leads to six-wave mixing, and phase-conjugation from four-wave mixing or "parametric diffraction".

There is a long history of research in the areas of stimulated backscatter and phase conjugation. A detailed theoretical and experimental study of stochastic backscatter has been performed by Shamonina et al.,[8] where it has been shown that a large local response such as in PR $LiNbO_3$ can stimulate a noisy backscatter. Amplification of the backscattered light in PR materials along the c-axis of the crystal has been reported in Refs [1-5]. References 3 and 4 report transient contra-directional self-phase conjugation due to stimulated backscatter in $LiNbO_3$:Fe. In this case, a strongly focused incident beam at nominally normal incidence on the crystal with its c-axis oriented opposite to the direction of propagation of the beam generates back reflection which contains the phase conjugate. A phase distorter which was inserted in the path of the incident beam originally to verify phase conjugation also optimized its quality (fidelity) by further increasing the divergence of the strongly focused incident beam.[3,4] Recently, strong stimulated backscatter leading to self-pumped phase conjugation has been observed in $LiNbO_3$:Mg at 351 nm where the PR sample exhibits large ultraviolet photorefractivity.[5]

For an obliquely incident pump, PR backscatter, and phase conjugation resulting from six-wave mixing have been demonstrated in PR $KNbO_3$:Fe [6,7]. In that case, the pump light is typically incident on the c-face of the crystal with an angle of about 10 degrees with respect to the c-axis, giving rise to beams traveling forward, backward, and normal to the interface, along with the phase conjugates. A transient contra-directional self-phase conjugation in PR $KNbO_3$ has also been observed using strongly focused beam at nominally normal incidence and a moving random phase plate.[4] In a separate PR material, such as $BaTiO_3$, self-pumped phase conjugation has been observed when the pump is obliquely incident on a crystal face other than the c-face, due to either corner-reflection[9] or generation of SPBS[10].

The quality of the phase-conjugate has been studied by various methods. The fidelity of phase conjugation resulting from amplification of Brillouin scattering has been quantitatively assessed through interferometric techniques.[11] In PR materials, the fidelity of a pair of phase conjugate beams has been monitored by measuring the visibility of fringes in interference experiments.[12]

For the benefit of readers, the implications of some of the terms used later in the paper will be briefly explained here. First, the term optical *beam* or *field* implies a collection of plane waves, as decomposed into its angular plane wave spectrum. The word *wave*, unless otherwise explicitly stated, implies a (*uniform*) *plane* wave. A *strongly focused* or *scattered beam* is therefore clearly not one plane wave, but a collection of many plane waves. Secondly, in PR wave mixing, two plane waves with complex amplitudes designated by C_i, C_j, whether incident independently or created from reflection from a boundary, scatter, etc., form an induced refractive index

proportional to $C_i^* C_j$ (and its complex conjugate). When the grating is simultaneously read out by C_i, the resulting diffracted wave ($\propto C_i C_i^* C_j$) loses the phase information of C_i and hence cannot be called its phase conjugate. This is called *self diffraction*[6,7], also commonly called *two-wave coupling (TWC)*. On the other hand, if a different wave, call that C_k, reads the grating, the corresponding diffracted wave ($\propto C_k C_i^* C_j$) contains the phase conjugate of C_i. This is called *parametric diffraction*[6,7], also commonly called *four-wave mixing (FWM)*. In this context, the work on phase conjugation in, for instance, $LiNbO_3$:Fe, using strongly focused beams and/or random phase plates [3,4] should be referred to as *two-beam* coupling or *multi-wave* mixing, since their strongly focused beam of 200 microns Rayleigh range has a divergence angle of approximately a few degrees, while the strongly focused beam passing through the random phase plate has a divergence angle six times as much.[3] In our case, we have conducted experiments using weakly focused beams with a waist of approximately 100 microns, which corresponds to divergence angles which are at least an order of magnitude smaller and therefore resembles a plane wave more closely.

In this paper, six-wave mixing in $LiNbO_3$:Fe, resulting from a 532 nm pump obliquely incident on the crystal and traveling nominally along the +c axis and with polarization perpendicular to the plane of incidence, which leads to SPBS, as well as beams traveling normal to the interface along the ±c axes, are investigated. The experimental procedure is summarized in Section 2. Randomly scattered light in some of these six directions may get amplified during self diffraction, or by coupling with light in other directions through parametric diffraction. The observed six-wave mixing is modeled using a set of coupled wave and material equations, as outlined in Section 3. The time dynamics of the six waves and the nature of SPBS are experimentally investigated for various $LiNbO_3$:Fe crystals (with different coatings, absorption coefficients and thicknesses) and for various incidence angles and powers of the pump. A novel order analysis for the steady state of the six waves is also presented in Section 3 and used to explain some of the experimental results, detailed in Section 4. The theoretical analysis clearly shows that the SPBS contains contributions from self diffraction and parametric diffraction. Since the latter contribution is proportional to the phase conjugate of the incident wave, as explained earlier, the SPBS is subjected to the classic image restoration test[9] for phase conjugates. Furthermore, the quality of the SPBS is investigated using interferometric methods, including measurement of the fringe visibility. Our experimental arrangement using weakly focused incident beam allows us to explicitly and independently monitor all six interacting waves which may contain self diffracted and parametrically diffracted contributions.

2. Experimental procedure

The observed six-wave mixing between waves $C_1 - C_6$ within the crystal can be understood using the schematic shown in Fig. 1. Scattered light in the six directions will have contributions from self diffraction or parametric diffraction, as will be clear from the theory in Section 3.

Iron doped lithium niobate crystals of various doping concentrations, coatings, and thicknesses are used as PR samples. The crystals and their different parameters are

presented in Table 1. All crystals have a cross-sectional area of 10 mm x 10 mm. In general, the experiments have been performed using crystal A; however, several supplementary experiments have been conducted using crystals B, C, D, and E. In particular,

(i) crystal B has been used to study the effect of higher Fe doping on six-wave mixing and SPBS;

(ii) crystal C, which is anti-reflection (AR) coated, has been used to study the effect of initial scatter upon reflection of the pump from the back surface of the crystal on six-wave mixing and SPBS;

(iii) crystal D, which is transparent conductive indium tin oxide (ITO) coated, has been used to study the effect of buildup of photovoltaic charges on six-wave mixing and SPBS; and

(iv) crystals B and E have been used to compare the effect of interaction length on six-wave mixing and SPBS.

Care is taken to remove gratings that build up in the crystals by subjecting them to a baking cycle, which involves heating them to 250 C and cooling them back to room temperature, between successive sets of measurements. Finally, to compare the SPBS from the $LiNbO_3$:Fe crystals with a standard phase conjugator, a 5 mm x 5 mm x 5 mm $BaTiO_3$:Ce crystal has been used as well.

2.1 Six-wave Mixing

The experimental arrangement to investigate six-wave mixing is shown in Fig. 2. The unexpanded 532 nm beam from a Verdi laser is focused with either a 750 mm or a 200 mm focal length lens (placed as L1) to waist sizes of 90 or 25 microns, respectively. The crystal is mounted on a rotation stage in order to study the dependence of the six-wave mixing on the angle of incidence of the pump, which is introduced nominally along the +c-axis and consequently opposite to the direction of the gain. The small angle, in air, between the pump propagation direction and c-axis is recorded. The crystal is placed at the focus and the pump beam is allowed to pass through a hole on screen S1 (see Figure 2). Screen S2 is placed behind the crystal to show all transmitted beams. The definitions of C_1-C_6 are in the caption of Fig. 1. For a 90 micron waist size beam, an incident power of 100 mW is used. We have found experimentally that for incident powers below 60 mW, six-wave mixing does not occur in any reasonable period of time. Using significantly more power causes photovoltaic noise,[13,14] which tends to wash out the SPBS (C_6) with each occurrence of the quasi-periodic photovoltaic breakdown.

The time evolutions of all interacting waves are monitored with a dual channel Newport 2832-C power meter and Newport 818-SL power detectors. Since only two beams can be recorded simultaneously, C_6 is kept common in all cases. Care is taken to reduce other scatter from being added to the SPBS by placing multiple irises along the path of C_6 (not shown on Fig. 2 for simplicity). The power in C_6 is detected after it is partially reflected off the second beam splitter BS2. All other beams (C_1-C_5) are detected by focusing them onto a second detector.

2.2 The nature of SPBS

As explained in the Introduction, since the observed SPBS C_6 consists of both self diffraction terms and parametric diffraction terms, the SPBS is expected to partially exhibit the nature of a phase conjugate. The SPBS from $LiNbO_3$:Fe is therefore subjected to the well-established image restoration test,[9] and compared with results from self-pumped phase conjugation from a $BaTiO_3$:Ce sample.

The nature of the SPBS from $LiNbO_3$:Fe is further investigated through the interference setup also shown in Fig. 2. A reference beam is derived from the pump beam by using a beam splitter (BS1). The reference beam is passed through an adjustable attenuator (combination of wave plate and polarizer) to make its power similar to that of the SPBS. Equal powers of the reference beam and SPBS are necessary to calculate the fringe visibility and extract information about the coherence of the SPBS. In the reference arm part of the interferometer, the pump beam is reflected with a mirror M1 after passing through the focusing lens L2.

For the first part of the interference experiment, when the crystal is placed at an arbitrary distance from lens L1, lens L2 is omitted. The motivation for this comes from the fact that a beam counter-propagating to the pump will not generate any circular fringes after retracing its path through an arbitrarily placed lens L1 and interfering with the collimated reference beam if and only if it is a perfect phase conjugate. This concept is first tested with a $BaTiO_3$:Ce crystal (a good phase conjugator), a plane mirror (which is not a phase conjugator and therefore expected to produce good fringes), and finally the $LiNbO_3$:Fe samples. In our experiment, the crystal is placed at a distance approximately *f*/2 behind L1 of focal length f=750 mm, and the pump power adjusted to maintain the in-focus intensity. For recording purposes, these fringes are expanded with a strongly focusing lens L3 (f = 50 mm) and projected on to screen S3. The fringe pattern on screen S3 is photographed with a 7 mega pixel digital camera (Sony DSC-W7). A variable neutral density filter is used to avoid saturation of the camera. Time evolution of the fringes is also monitored.

In the second part of the interference experiment (coherence test), both the $LiNbO_3$:Fe crystals and the plane mirror described above are placed at the focus of the lens L1. Placing the crystals and the mirror at the focus results in a collimated beam after it propagates back through the lens L1. The second lens L2 (f = 750 mm) is now inserted to introduce phase curvature. Circular fringes generated using this interference procedure are recorded with the digital camera. Fringe visibility is calculated for both cases from the interference pictures using MathCAD in order to quantify the quality of the interference fringes, and hence to infer the quality of the phase conjugate generated using $LiNbO_3$:Fe.

3. Theory

The observed six-wave mixing can be modeled using the schematic shown earlier in Fig. 1. Scattered light in these six directions may get amplified by self diffraction or by parametric diffraction. Considering reflection gratings only, from Maxwell's equations the following coupled equations can be derived for the complex amplitudes C_m $(m = 1,...,6)$ of the interacting optical fields nominally propagating in the directions 1-6 shown in Fig. 1 inside the PR material:[7]

$$L_1C_1 = n_{12}C_2 + n_{13}C_3 + n_{16}C_6 + n_{46}C_3 + n_{56}C_2 \quad (1.1)$$

$$L_2C_2 = n_{21}C_1 + n_{24}C_4 + n_{25}C_5 + n_{65}C_1 + n_{35}C_4 \quad (1.2)$$

$$L_3C_3 = n_{31}C_1 + n_{34}C_4 + n_{35}C_5 + n_{64}C_1 + n_{24}C_5 \quad (1.3)$$

$$L_4C_4 = n_{42}C_2 + n_{43}C_3 + n_{46}C_6 + n_{53}C_2 + n_{13}C_6 \quad (1.4)$$

$$L_5C_5 = n_{52}C_2 + n_{53}C_3 + n_{56}C_6 + n_{12}C_6 + n_{42}C_3 \quad (1.5)$$

$$L_6C_6 = n_{61}C_1 + n_{64}C_4 + n_{65}C_5 + n_{21}C_5 + n_{31}C_4 \quad (1.6)$$

where L_m are dimensionless operators defined as $L_m = (\nabla_{Tm}{}^2 + 2jk_{z_m}\partial/\partial z_m)/k_0{}^2$; $k_0 = 2\pi/\lambda$ is the wave number in the crystal, λ is the optical wavelength in the crystal, and k_{z_m} is the propagation constant of the m-th field ($m = 1,...,6$) along its nominal propagation direction m. Also, $\nabla_{Tm}{}^2$ is the Laplacian in the plane transverse to the nominal direction of propagation of the m-th field. In our reported experiments, the angles between the various interacting fields are no greater than 3 degrees inside the crystal; furthermore, due to *weak* focusing, all interacting fields can be approximately regarded as quasi-plane waves, implying minimal propagational diffraction within the interaction region. The spatial amplitudes of the dielectric permittivity grating n_{ij} formed from nominally counter-propagating interacting fields C_i, C_j can be found from material equations and a standard photorefractive band-transport model[6] as:

$$\tau_{ij}\partial n_{ij}/\partial t = \gamma_{ij}C_iC_j^* - \beta_{ij}n_{ij} \quad (2)$$

where $n_{ij} = n_{ji}{}^*$, τ_{ij} denotes the Maxwell relaxation time, and parameters γ_{ij}, β_{ij} depend on crystal symmetry. As stated above, only reflection gratings are considered, since transmission gratings have wavevectors for which the electro-optic coefficients are much smaller. Similar optical and material equations appear in Korolkov et al.[4] and references therein, with the difference that in their paper, propagation of, and interactions between, the *composite* forward and backward traveling optical fields are modeled. Using (2), the first three terms in each equation in (1) represent self diffraction terms, while the last two terms represent parametric diffraction. The last equation in (1) that signifies the spatial evolution of the SPBS is illustrated in Fig. 3, where the scattering diagrams explicitly show grating formation and readout for self diffraction and parametric diffraction.

In what follows, it is shown that a heuristic order analysis of Eqs. (1.1-1.6) along with (2) can give further insight into the nature of various interacting waves and how they are formed. Although heuristic, inferences from this order analysis can explain some of our experimental results, as described in the following Section. One can assign book-keeping parameters δ to the reflection coefficient, and ε to the backscattering. If C_1 is assigned the order $\delta^0\varepsilon^0$, then C_2, to a first approximation, would be of order $\delta^1\varepsilon^0$ since it is generated by the reflection of C_1 from the back surface of the crystal. The wave C_3, presumably generated by the backscatter of C_1 upon reflection from the back surface, would be of order $\delta^1\varepsilon^1$, while C_4 formed by the reflection of C_3 from the front surface

would have order $\delta^2\varepsilon^1$. Such order assignments cannot be done for C_5 and C_6 since these are exclusively generated through parametric diffraction and amplified through self diffraction. With the initial assigned orders for the waves C_1-C_4, it can be shown from Eq. (1.6), along with the steady state limit of Eq. (2): $n_{ij} \propto C_i C_j^*$, that C_6 could have the next higher order $\delta^3\varepsilon^2$ arising from the order of the last term $n_{31}C_4$ on the RHS which represents parametric diffraction. With this assumption, it is observed that the first term $n_{61}C_1$ in Eq. (1.6) representing self diffraction also has the same order. A similar order analysis for C_5 based on Eq. (1.5) shows that its dominant order is $\delta^4\varepsilon^2$ arising from the terms $n_{12}C_6$ and $n_{42}C_3$. Using this, it is observed that the next higher order, viz. $\delta^5\varepsilon^2$ in Eq. (1.6) is the term $n_{21}C_5$. It turns out that this term is non-negligible under certain experimental conditions, to be described later. In a similar way, all the other equations (1.1)-(1.5) can be revisited, and terms up to two orders higher in δ and one order higher in ε retained. This results in the reduced set of equations (3.1)-(3.6) below:

$$L_1C_1 = n_{13}C_3(O:\delta^1\varepsilon^0) + n_{12}C_2(O:\delta^1\varepsilon^1) \quad (3.1)$$

$$L_2C_2 = n_{21}C_1(O:\delta^1\varepsilon^0) \quad (3.2)$$

$$L_3C_3 = n_{31}C_1(O:\delta^1\varepsilon^1) \quad (3.2)$$

$$L_4C_4 = n_{42}C_2(O:\delta^4\varepsilon^1) \quad (3.4)$$

$$L_5C_5 = (n_{12}C_6 + n_{42}C_3)(O:\delta^4\varepsilon^2) + n_{52}C_2(O:\delta^6\varepsilon^2) \quad (3.5)$$

$$L_6C_6 = (n_{61}C_1 + n_{31}C_4)(O:\delta^3\varepsilon^2) + n_{21}C_5(O:\delta^5\varepsilon^2) \quad (3.6)$$

One of our objectives in this paper is to determine the nature of C_6. As seen from Eq. (3.6), C_6 contains contributions from (a) self diffraction ($n_{61}C_1$), and (b) parametric diffraction ($n_{31}C_4$ and $n_{21}C_5$), which contain the phase conjugate of C_1 as stated earlier in the Introduction. This will have relevance in a later section of this paper where the nature of SPBS is investigated using interferometric techniques.

Equation (3.1) suggests that as C_1 self diffracts, it couples its power to C_2 and C_3, as also evidenced from Eqs. (3.2) and (3.3). It should be noted that additional factors, also significantly affecting C_3, are not included in the above theory. For instance, C_3 points in the direction of the gain, which gives C_3 an advantage over other participating waves when it comes to coupling power into the waves. In addition, C_3 and C_4 may also grow due to Fabry-Perot effect under the right conditions, where the reflected scatter from the pump is amplified along the gain direction. Furthermore, the angle between the pump and the *c*-axis also affects the growth of all six-waves, since two-beam coupling efficiency diminishes with increasing angle (i.e., decreasing overlap). This is most significant for C_3 since it primarily acquires power from C_1 (Eq. 3.3) through self diffraction. The same statement is also true for C_2, as it also gains power mostly from C_1 (Eq. 3.2) through self diffraction. The relevance of this discussion will be clear below when experimental results on six-wave mixing are presented.

4. Results and Discussions

4.1 Six-wave Mixing

Figure 4 shows photographs of the intensity patterns observed on screen S1 before and after C_3 is formed for an incident angle of 4 degrees (in air) using crystal A. The pump power is 100 mW and is focused by L1 of focal length f=750 mm to a spot size of 90 microns. Initial brightness in the direction of C_2 comes from the instantaneous Fresnel reflection from the crystal surface. The light around the hole on screen S1 (through which the incident beam is introduced) is only from the SPBS C_6. It is observed that C_6 generally forms between 100 ms -10 s after the pump beam is turned on, as further discussed below. Similar photographs of intensity patterns observed on screen S2 have been also recorded, but not shown here for the sake of brevity. It is observed that all participating waves maintain the same polarization (which is vertical, and hence perpendicular to the plane of incidence) as the incident pump. The typical generation times for C_3 and C_4, propagating along the ± c- axes, are of the order of a few seconds for the incident angle and the pump power used in the experiment. A careful monitoring of C_3 and C_4 sometimes reveals the presence of a hexagonal structure. This is in agreement with previous observations of hexagon formation for normal and oblique incidence using $KNbO_3$:Fe,[6] and for normal incidence using $LiNbO_3$:Fe and a feedback mirror.[15] It has been shown that the hexagonal formation in C_3 and C_4 is from amplification and self-organization of light initially scattered into Fabry-Perot modes.[6]

The formation of Fabry-Perot modes is influenced by

(a) the amount of scatter in the direction of C_3 and C_4, and

(b) the interaction length between the participating waves.

Hypothesis (a) is supported by the following observations:

(i) increasing the angle of incidence of the 100 mW pump above a certain critical angle, viz., 8 degrees (in air) for crystal A, inhibits formation of C_3 and C_4, for a focused spot size of 90 microns;

(ii) using crystal C, which is anti-reflection coated, and thus has very low reflection coefficient and accordingly low initial scattering along C_3, yields intensities of C_3 and C_4 which are an order of magnitude smaller than that observed using crystal A for the same incident power, angle, and pump spot size.

Note that under identical conditions, using crystal B, which has higher dopant concentration, yields intensities of C_3 and C_4 which are comparable to that observed for crystal A. The reason for this is that although crystal B has larger Fe concentration than crystal A and hence has higher gain, the absorption in crystal B is also correspondingly higher (see Table 1).

Hypothesis (b) is supported by the following observations:

(i) using a shorter crystal, viz., crystal E, of thickness 5 mm (see Table 1), the intensities of C_3 and C_4, and SPBS C_6, are typically an order of magnitude smaller than what is observed for crystal B;

(ii) experimentation with a more tightly focused 25 micron 100 mW beam (using lens L1 of focal length 200 mm) shows that the critical incident

angle to generate C_3 and C_4 decreases to 2 degrees for crystal A. This is because with a smaller spot size, there is less effective interaction length between the participating beams to initiate the growth of C_3 and C_4.

We would like to comment that both hypotheses (a) and (b) are supported by the results in Kukhtarev et al.,[7] which show that the threshold condition for observation of light in the directions of C_3 and C_4 is determined by the magnitude of the "seeding scattering parameter" and the effective interaction length. Antireflection coating reduces the seeding scattering, while larger angles and smaller waists, or shorter crystal, reduce the interaction length.

The time dynamics of six-wave mixing using crystal A for a duration of 10 minutes are shown in Figure 5 for an incidence angle of 4 degrees (in air), pump power of 100 mW and pump spot size of 90 microns. The observations and pertinent discussion are summarized below:

(a) **Steady state powers**: For crystal A, the SPBS (C_6) power is around 60 microwatts averaged over the five sets of measurements of the powers in C_1 through C_5 (see Figure 5), as explained in Section 3.1. For completeness, SPBS powers for all crystals (A-E) have been tabulated in Table 1. Also, Figure 5 shows that the powers in C_4, C_5, and C_6 (in the order of hundred microwatts) are an order of magnitude lower compared to C_1, C_2 and C_3 (tens of milliwatts). These observations are in agreement with our theory, since according to Eqs. (3.1-3.6), C_1, C_2 and C_3 have much lower orders of δ, ε compared to that of C_4, C_5, and C_6. A consequence of this is that temporal fluctuations around the steady state are more noticeable for the lower power waves, viz., C_5, and C_6.

(b) **Temporal behavior**: The SPBS C_6 may show two time scales during its formation. We have found, after carefully examining 24 traces of the generation of C_6, that in 16 cases, an initial rise in C_6 was observed within a characteristic time of 100 ms, followed by a slower rise with a characteristic time of a few seconds. In the remaining 8 cases, only the slower rise time was observed. Note that in Fig. 5, the observed initial "jump" in C_6 results from averaging over 5 traces, of which 4 had the faster time response. After the initial fast response of C_6, it is observed that C_3, C_4, and C_5, also form within a few seconds after the pump beam is turned on. While the *linear Fresnel-reflected* intensity of the incident light from the crystal interface in the direction of C_2 is instantaneous (as seen from the sharp initial jump), the nonlinearly generated C_2 evolves at a time scale similar to the longer rise time of C_6. Also, as C_1 and C_3

reach steady state, C_6 attains steady state as well. This is in agreement with our heuristic theory since from Eq. (3.6), it is observed that the nature of C_6 at or near steady state should be primarily determined from the nature of the first two terms on the right hand side since these are of lower order in δ, ε. When Fabry-Perot modes leading to amplification of C_3, and hence C_4, are supported, the behavior of C_6 should also depend on the combined behavior of C_1, C_3 and C_4. As C_1, C_3 and C_4 reach steady state, C_6 is therefore expected to reach steady state as well. The occasional initial sharp rise in C_6 can be heuristically explained by noting that the initial evolution of C_6 in the absence of C_3, C_4 and C_5 depends on $n_{61}C_1$; so that in the presence of the pump C_1 and occasional *stronger* scatter in the direction of C_6 (depending on where the incident light falls on the crystal), there may be enough self diffraction to produce the initial faster evolution of SPBS.

(c) **Photovoltaic noise**: Some of the participating waves show periodic flashes (spikes in power) (see Figure 5). The frequency of spikes is much higher for the darker crystal B (not shown here for the sake of brevity), occurring simultaneously at approximately every 50 sec. for all of the six participating waves. In contra-directional two-beam coupling these flashes have been attributed to destruction of the grating owing to photovoltaic breakdown.[13,14] It is observed that in crystal B, because of photovoltaic breakdown, C_2, C_3, C_6 show a decrease in power (down spike, not shown) while C_1, C_4, and C_5 correspondingly show an increase in power (up spike). Since it has been shown that the photovoltaic noise can be reduced by ITO coating the crystal,[13,14] the six-wave mixing experiment has been repeated using the ITO coated crystal D (see Table 1). The time dynamics (not shown here) show that photovoltaic pulsations in all participating waves are, in fact, eliminated in the ITO coated crystal.

(d) **Dependence on angle of incidence**: The average SPBS power does not change with the angle of incidence up to 30 degrees, when C_3 and C_4 do not form. On average, the power in C_6 is similar to the $\theta = 4$ degrees case shown in Fig. 5 and of the order of 60 microwatts.

4.2 The nature of SPBS

As stated in Section 3.2, the nature of SPBS is investigated using imaging and interferometric methods. The results and pertinent discussion are summarized below:

(a) **Image restoration**: It is observed that while $BaTiO_3$:Ce recreates the image of the Air Force Resolution Chart clearly, crystals A and B yield at best fuzzy images of the resolution chart where the images cannot be seen clearly. This is in agreement with our theory which shows that SPBS has contributions from self diffraction and parametric diffraction

(Eq. (3.6)), with only parametric diffraction contributing to the phase conjugation of the incident wave(s).

(b) **Interference of SPBS with the collimated pump**: With the $BaTiO_3$:Ce sample and crystal B deliberately positioned at approximately *f*/2 behind lens L1 to introduce arbitrary phase curvature, the resulting observations are presented in Fig. 6. The SPBS from $BaTiO_3$:Ce after retracing its path emerges collimated and does not produce any concentric rings when it is interfered with the collimated pump (see Fig. 6a). The absence of circular fringes is not due to lack of coherence, as evident from the linear fringes (shown in the inset) that results when the reference beam is slightly tilted. Figure 6b shows the stable concentric fringes that result when the pump beam is reflected by a mirror from the same position *f*/2 behind L1. When the crystal B is placed at the same distance behind L1, the circular fringes do appear (Fig. 6c) and tend to be very unstable. It is observed that fringes appear within a minute after the pump is turned on (when the SPBS first appears). Although the total SPBS power is approximately constant, the fringes appear and disappear aperiodically over a time scale of approximately 5 minutes.

The lack of fringes in the case of $BaTiO_3$:Ce should be from phase conjugation[1] through parametric diffraction. The circular fringes observed when using a mirror are due to the phase curvature introduced from the lens L1. For the case of $LiNbO_3$:Fe, the SPBS comprises both self diffraction and parametric diffraction, and there is a continuous exchange of power between the parametrically diffracted and self diffracted backscatter as observed from the absence and presence of fringes.

(c) **Coherence test**: As discussed in Section 3.2, the quality of SPBS and the contribution of parametric diffraction in $LiNbO_3$:Fe is assessed by recording the fringes obtained using crystal B (Fig. 7a) and a plane mirror (Fig. 7b) for comparison. Fringe visibility is then calculated using $V = (I_{max} - I_{min})/(I_{max} + I_{min})$.[16] Since the SPBS fringes from sample B do not have uniform visibility, a vertical cut through the center of the figure has been taken since it shows better contrast than a horizontal cut. For the mirror, V = 0.65, while for the SPBS using sample B, V = 0.30 upon choosing the second and third peaks on the left of the center peak on the vertical cuts (Fig. 7c). It is speculated that the decreased visibility is from the contribution of self diffraction in SPBS. Combination of self diffracted light and parametrically diffracted light, which is phase-conjugate of C_1, reduces the overall coherence of the SPBS C_6, but does not destroy it completely.

It is proposed that reduction of self diffraction, through use of a tightly focused pump,[17] or application of external field along with large Fe^{2+} doping,[18] or through grating translation by piezoelectrically induced low frequency vibrations in the crystals,[18] may significantly improve the phase conjugate in SPBS in the six-wave mixing geometry. In the contra-directional beam coupling geometry, where the pump is normally incident on

the crystal and the c-axis is oriented opposite to the direction of propagation, it has already been shown that only a very tightly focused pump results in transient phase-conjugate reflection.[3,4]

5. Conclusion

Six-wave mixing in different samples of $LiNbO_3$:Fe with various concentrations, coatings and thicknesses has been investigated for oblique incidence of a 532 nm pump with respect to the c-axis. It is shown that the generated SPBS contains contributions from self diffraction and parametric diffraction, the latter containing the self-phase conjugate of the pump. A consequence of six-wave mixing is the generation of waves (and, sometimes, hexagonal patterns) traveling along the ±c axes, whose intensities depend on the amount of scatter along the ±c axes and the interaction length of the six waves in the crystal. The time dynamics and the steady states for all participating waves have been experimentally studied and reconciled with inferences from approximate heuristic theory. A careful study of the SPBS, which includes image restoration test, interference with the pump, and visibility measurement, suggests that the phase conjugation may be contaminated by the self diffraction. It is postulated that reduction of self diffraction may significantly improve the phase conjugate in SPBS.

References

1. I. F. Kanaev, V. K. Malinovski, and B. I. Sturman, "Induced reflection and bleaching effects in electro-optic crystals," Sov. Phys. JETP **47**, 834-837 (1978).
2. G. Valley, ''Evolution of phase-conjugate waves in stimulated photorefractive backscattering,'' J. Opt. Soc. Am. A **9**, 1440-1448 (1992).
3. A.V. Mamaev and V.V. Shkunov, "Transient phase self-conjugation in a lithium niobate crystal", Sov. J. Quant. Elec. **18** 829-830 (1988).
4. S.A. Korolkov, A.V. Mamaev and V.V. Shkunov, "Stimulated diffusion backscattering with phase conjugation", Int. J. Nonlinear Opt. Phys. **2** 157-169 (1993), and references therein.
5. H. Qiao, Y. Tomita, J. Xu, Q. Wu, G. Zhang, and G. Zhang, "Observation of strong stimulated photorefractive scattering and self-pumped phase conjugation in $LiNbO_3$:Mg in the ultraviolet", Opt. Express **13**, 7666-7671 (2005).
6. N. V. Kukhtarev, T. Kukhtareva, H. J. Caulfield, P. Banerjee, H.-L. Yu, and L. Hesselink, "Broadband dynamic, holographically self recorded, and static hexagonal scattering patterns in photorefractive $KNbO_3$:Fe," Opt. Eng. **34**, 2261-2268 (1995).
7. N. Kukhtarev, T. Kukhtareva, R. Jones, J. Wang, and P. Banerjee, "Real-time holography for optical processing using photorefractive crystals," Photorefractive Fiber and Crystal Devices: Materials and Optical Properties IX, Proc. SPIE **3793**, 90-96 (1999).
8. E. Shamonina, B. I. Sturman, S. G. Odoulov, and K. H. Ringhofer, "Investigation of stochastic photorefractive backscattering," J. Opt. Soc. Amer. B **13**, 2242-2251 (1996).
9. J. Feinberg, "Self-pumped, continuous-wave phase conjugator using internal reflection," Opt. Lett. **7**, 486-488 (1982).
10. P. Buranasiri, P. P. Banerjee, V. Polejaev, and C. C. Sun, "Image correlation using isotropic and anisotropic higher-order generation and mutually pumped phase conjugation in photorefractive barium titanate," Photorefractive Fiber and Crystal Devices: Materials, Optical Properties, and Applications IX, Proc. SPIE **5206**, 215-222 (2003).
11. P. Suni and J. Falk, " Measurements of stimulated Brillouin scattering p hase-conjugate fidelity," Opt. Lett. **12**, 838-840 (1987).
12. M.D. Ewbank, "Mechanism for photorefractive phase conjugation using incoherent beams," Opt. Lett. **13**, 47-49 (1988).
13. D. R. Evans, S. A. Basun, M. A. Saleh, T. P. Pottenger, G. Cook, T. J. Bunning, and S. Guha, "Elimination of photorefractive grating writing instabilities in iron-doped lithium niobate," IEEE J. Quantum. Elec. **38**, 1661-1663 (2001).
14. D. R. Evans, J. L. Gibson, S. A. Basun, M. A. Saleh, and G. Cook, "Understanding and eliminating photovoltaic induced instabilities during contra-directional two-beam coupling in photorefractive $LiNbO_3$:Fe," Opt. Mat. **27**, 1730-1732 (2005).
15. S. Odoulov, B. Sturman and E. Kratzig, "Seeded and spontaneous light hexagons in $LiNbO_3$:Fe", Appl. Phys. B **70,** 645-647 (2000).
16. E. Hecht, *Optics*, Addison-Wesley, New York (1987).
17. G. Cook, D. C. Jones, C. J. Finnan, L. L. Taylor, and T. W. Vere, "Optical limiting with lithium niobate," Power Limiting Materials and Devices, C. M. Lawson, ed., Proc. SPIE **3798,** 2-16 (1999).
18. M. Lueneemanna, K. Buse, and B. Sturman, "Coupling effects for counterpropagating light beams in lithium niobate crystals studied by grating translation technique for extremely high electric fields", J. Appl. Phys. **94,** 6274-6279 (2003).

Figure Captions

Fig. 1. Schematic representation of the six waves inside the crystal. C_1 denotes the forward propagating pump through the crystal. C_2 represents the result of six-wave mixing in the direction of the Fresnel reflection of the pump from the surface. C_3 and C_4 denote the waves generated in the crystal that are perpendicular to the interface, and consequently along the *c*-axis. C_5 and C_6 (the SPBS) make up the other two participating waves in the six-wave mixing scheme.

Fig. 2. Schematic representation of the experimental arrangement. L1-L3: lenses; M1, M2: mirrors; BS1, BS2: beam splitters. The pump is collimated 532 nm light from a Verdi laser. Six-wave mixing is observed on screens S1 and S2. Lens L1 is used to focus the pump onto the PR sample which is placed at its back focus for six-wave mixing experiments. SPBS (C_6) power is measured with the detector shown. Powers in $C_1 - C_5$ are also recorded with similar detectors placed directly in the path of the beams after exit from the crystal in their respective directions. Lens L3 and screen S3 are used during interference experiments for determination of the quality of SPBS. The PR sample is first placed at an arbitrary distance from lens L1 and the SPBS interfered with a portion of the collimated pump reflected by the mirror M1 with lens L2 removed. Thereafter, the sample is reinserted at the back focal plane of L1 and the interference of the SPBS with a portion of the pump focused by L2 and reflected by the mirror M1 is monitored.

Fig. 3. Calculation of contributions to SPBS (C_6) using scattering diagrams, following Eq. (1.6). The thin lines on the right hand side refer to k-vectors of waves participating in the grating, while the dark lines represent the k-vector of the wave reading the grating.

Fig. 4. (a) Backscattered beam C_6 and linearly reflected light in the direction of C_2. While the latter is instantaneously generated, C_6 forms between 100 ms-10 s after the pump beam is turned on. The pump beam, in the direction of C_1 passes through a hole on screen S1. (b) Subsequent generation of C_2 and C_3 is seen on screen S1. The bright spot along C_2 also includes the instantaneously generated Fresnel reflected light.

Fig. 5. Time dynamics of six-wave mixing for crystal A at an angle of incidence of 4 degrees (in air) for the pump. Screens S1 and S2 in Fig. 2 are replaced by detectors and C_1-C_5 are focused onto the detectors. The beams are recorded in pairs, with C_6 being common in all cases. The average of all five C_6 traces is shown.

Fig. 6. Interference with the reference (pump) when the crystal (or the mirror) is placed at a distance approximately $f/2$ from lens L1. (a) Interference pattern between the reference and the phase conjugate from $BaTiO_3$:Ce. Note the absence of circular fringes due to phase correction from phase conjugation. Inset shows linear fringes when the mirror M1 which reflects the reference is tilted. (b) Interference between the reference and reflection from a plane mirror placed at the location of the crystal. (c) Interference pattern between the reference and the SPBS from $LiNbO_3$:Fe.

Fig. 7. Quantification of the coherence of the SPBS through visibility measurement from interference patterns. (a) Interference pattern between the reference and the SPBS from $LiNbO_3$:Fe. (b) Interference pattern between the reference and a reflection from a plane mirror placed at the location of the crystal). (c) Intensity patterns along a vertical cut through both interference patterns recorded in (a) and (b), which is used for visibility calculations.

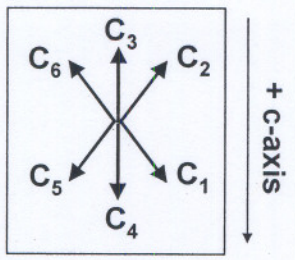

Figure 1

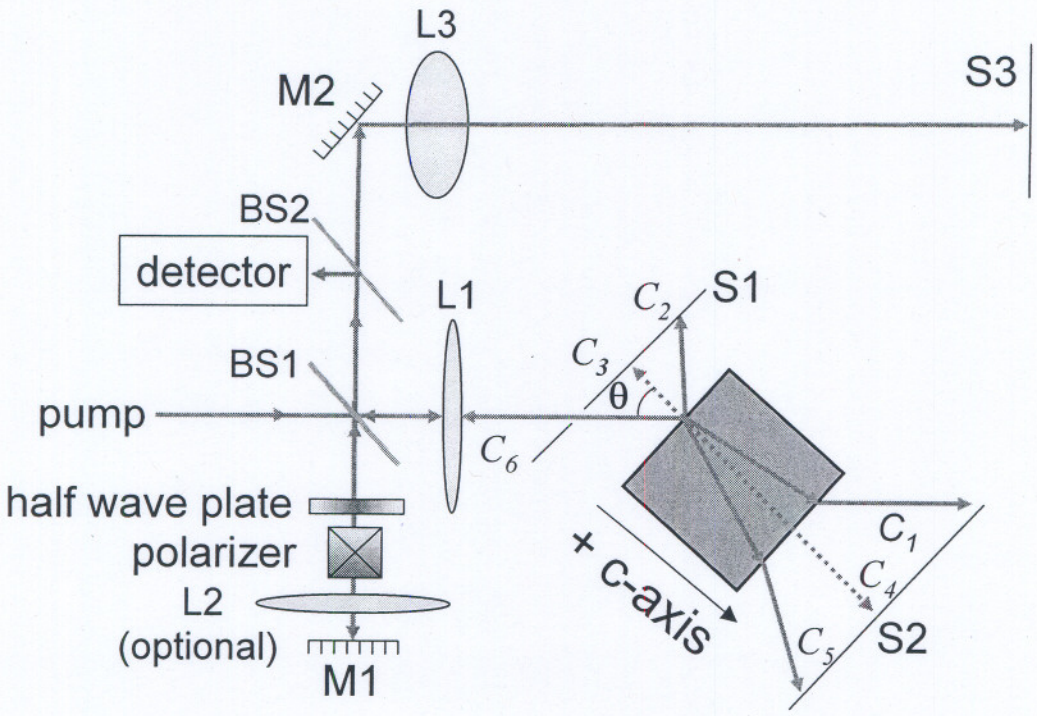
L3
M2
S3
BS2
detector
L1
C_2
S1
C_3
θ
BS1
pump
C_6
half wave plate
polarizer
L2
(optional)
M1
+ c-axis
C_1
C_4
C_5
S2

Figure 2

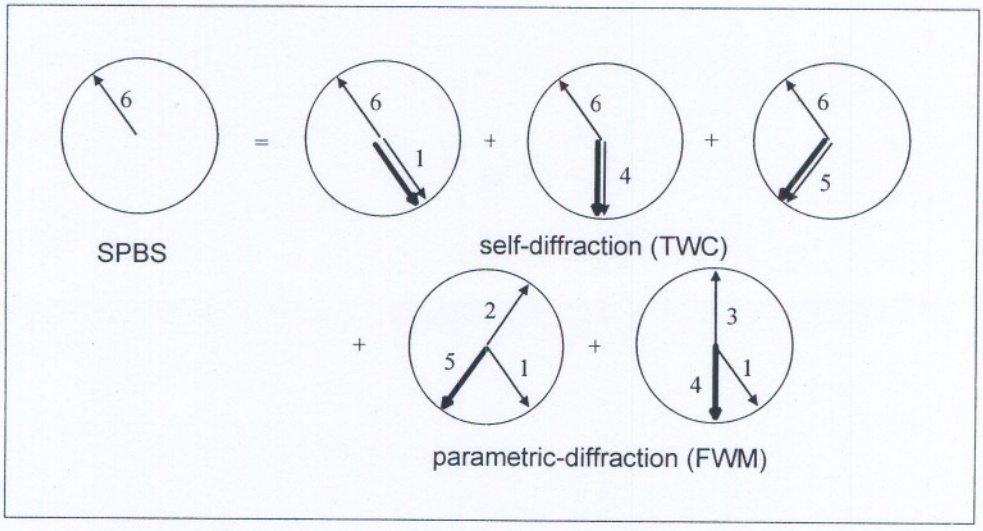
6
=
6
1
+
6
4
+
6
5
SPBS
self-diffraction (TWC)
+
2
5
1
+
3
4
1
parametric-diffraction (FWM)

Figure 3

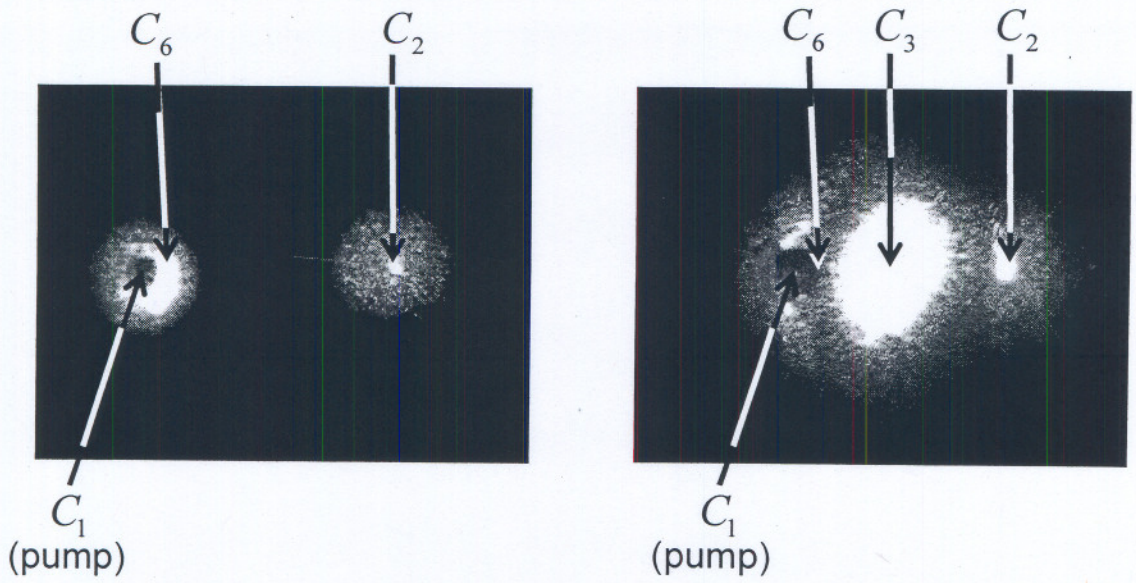

(a) **(b)**

Figure 4

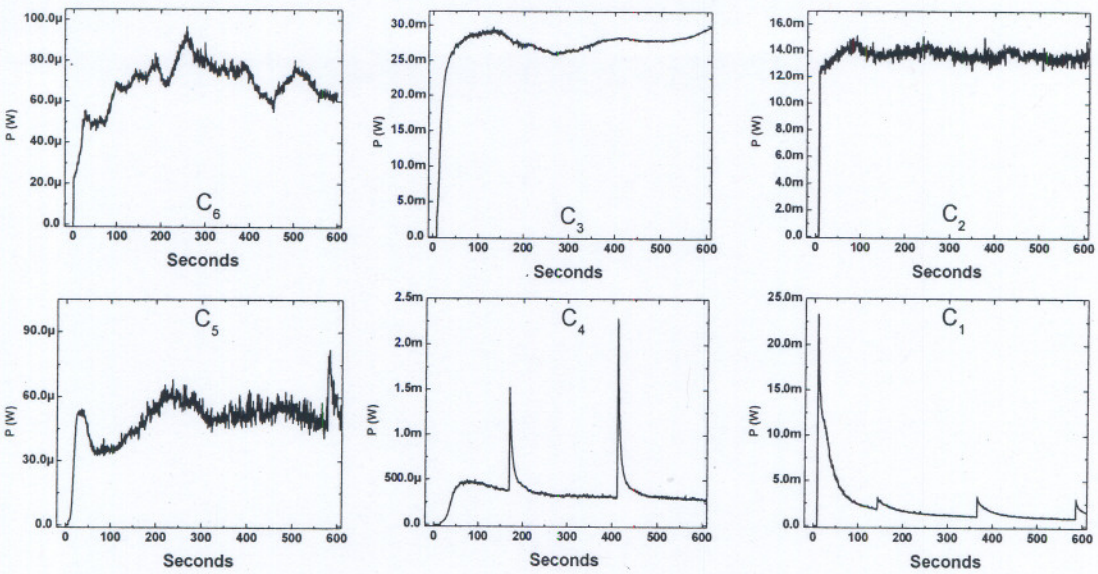

Figure 5

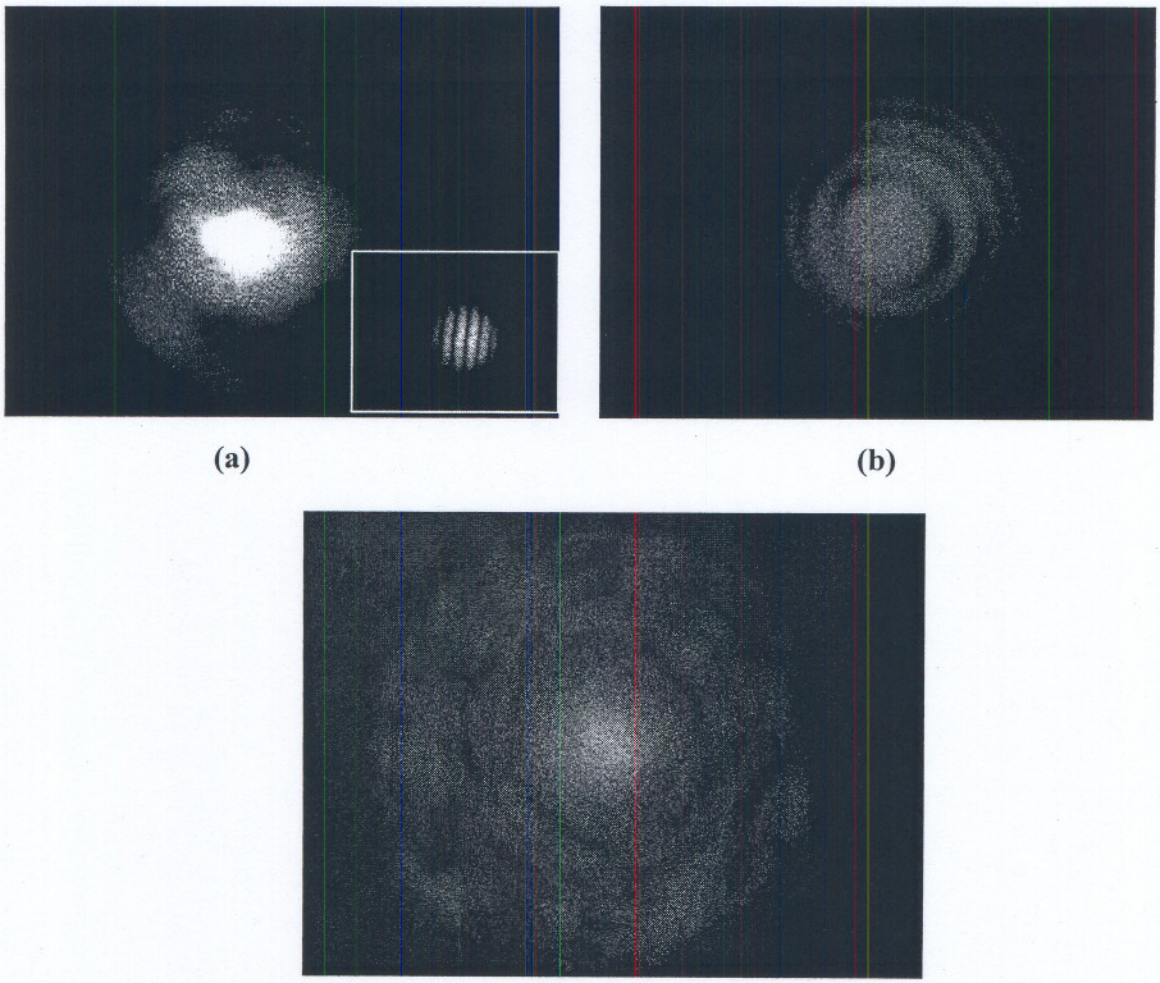

(a) **(b)**

(c)

Figure 6

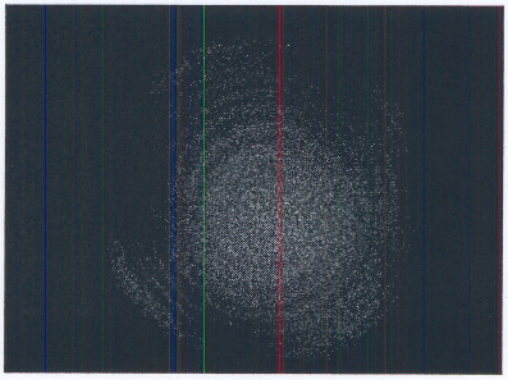

(a)

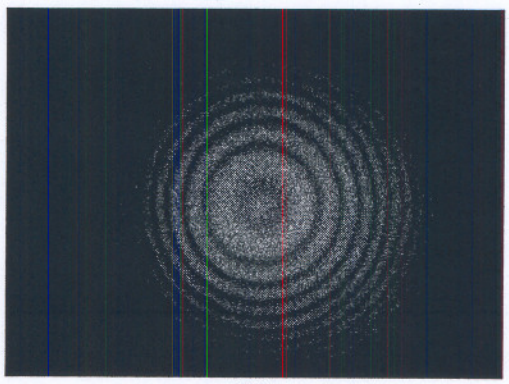

(b)

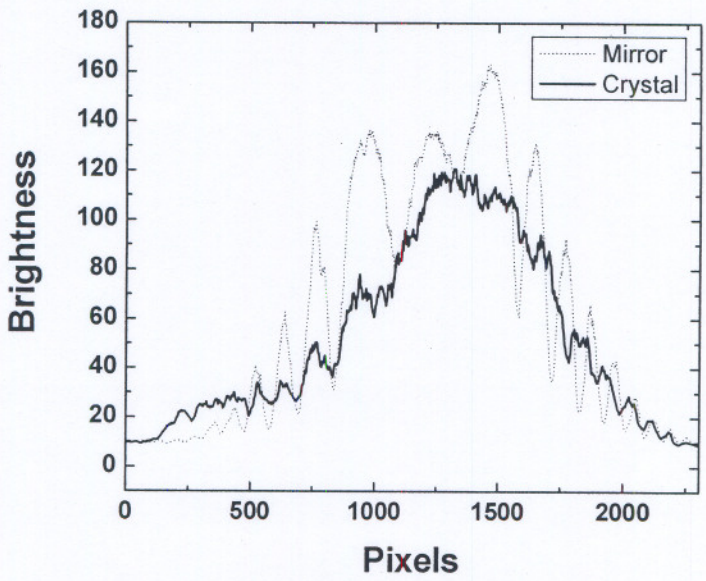
Brightness
Pixels
Mirror
Crystal
0
20
40
60
80
100
120
140
160
180
0
500
1000
1500
2000

(c)

Figure 7

Table 1. Relevant parameters for all the $LiNbO_3$:Fe crystals used.

crystal marked	mol % Fe_2O_3 in the melt	c-axis (mm)	coatings on z-surfaces	absorption coefficient (cm^{-1})	SPBS at 4° incidence (μW)
A	0.03	10	none	0.43	60
B	0.05	10	none	1.20	20
C	0.03	10	AR	0.47	4
D	0.05	10	ITO	1.17	20
E	0.05	5	none	1.19	5

ITO: conducting coating of indium tin oxide. AR: Anti-reflection coating. The last column compares steady state SPBS powers for the various crystals.